An Operational Evaluation of Two Regional-Scale Ozone Air Quality Modeling Systems over the Eastern United States

Gopal Sistla,* Winston Hao,* Jia-Yeong Ku,* George Kallos,+
Kesu Zhang,# Huiting Mao,# and S. Trivikrama Rao#

ABSTRACT

In this paper, the performance of two commonly used regional-scale Eulerian photochemical modeling systems, namely, RAMS/UAM-V and MM5/SAQM, from the regulatory or operational perspective, is examined. While the Urban Airshed Model with Variable Grid (UAM-V) is driven with the meteorological fields derived from the Regional Atmospheric Model System (RAMS), the San Joaquin Valley Air Quality Model (SAQM) used the meteorological fields derived from the Pennsylvania State University–National Center for Atmospheric Research Mesoscale Model Version 5 (MM5). The model's performance in reproducing the observed ozone air quality over the eastern United States is evaluated for three typical high-ozone episodic events that occurred during 16–20 June, 12–16 July, and 30 July–2 August of 1995. The prevailing meteorological conditions associated with these three episodes are characterized by a slow eastward-moving high pressure system, westerly and southwesterly low-level jets, stable boundary layers, and the Appalachian lee-side trough. The results suggest that the performance of RAMS/UAM-V and MM5/SAQM systems in reproducing the observed ozone concentrations is comparable when model outputs are averaged over all simulated days. For different emissions reduction (i.e., volatile organic compound and nitrogen oxide controls) options, the response of both modeling systems, in terms of changes in ozone levels, was directionally similar, but the magnitude of ozone improvement differed from individual episode days at individual grid cells.

1. Introduction

Summertime ozone levels in many parts of the eastern United States continue to exceed the 1-h ozone National Ambient Air Quality Standard (NAAQS) of 0.12 ppm, posing a health risk to urban population centers. Also, the shift to the 8-h average standard (EPA 1997) is expected to greatly expand the spatial extent of the ozone problem in the eastern United States (Chameides et al. 1997). The work by the Ozone Transport Assessment Group (OTAG) demonstrated that the ozone problem is not limited to urban areas but has a strong regional component extending over distances of 1000 km or more (OTAG 1997). Also, trajectory-clustering and time-lagged intersite correlation techniques, as well as statistical analyses of ambient ozone data, revealed the regional nature of ozone in the eastern United States and the associated spatial and temporal sales associated with the ozone processes (Clarke and Ching 1983; Lyons and Cole 1976; Brankov et al. 1998; Rao et al. 1997).

Under the regulatory framework, areas not meeting the ozone NAAQS are required to demonstrate through an appropriate planning process that adequate steps, such as reductions in anthropogenic emissions of ozone precursors, will be undertaken to mitigate the ozone problem. Such an analysis is often pursued

*Division of Air Resources, New York State Department of Environmental Conservation, Albany, New York.
+Department of Applied Physics, University of Athens, Athens, Greece.
#Department of Earth and Atmospheric Sciences, the University at Albany, State University of New York, Albany, New York.
Corresponding author address: Dr. S. T. Rao, Office of Science and Technology, New York State Department of Environmental Conservation, 50 Wolf Rd., Albany, NY 12233-3259.
E-mail: strao@dec.state.ny.us
In final form 21 November 2000.

through the use of grid-based photochemical models, since they are designed to simulate the complex physical and chemical processes associated with the production and removal of ozone. Using meteorological data that are representative of historical ozone episodes, future ozone air quality stemming from changes in precursor emissions is predicted by the grid-based photochemical models. This approach has been widely accepted, and several photochemical grid models are now available to assess current and future ozone air quality (Russell and Dennis 2000). However, depending upon the formulation of meteorological fields, numerical algorithms, and parameterization schemes used in simulating the ozone process, these models could give rise to differences in the modeled ozone concentrations that could, in turn, affect the efficacy of emission control strategies.

The objectives of this study are to examine the performance of two modeling systems, RAMS/UAM-V [Regional Atmospheric Model System (Pielke and Uliasz 1998) and Urban Airshed Model with Variable Grid (SAI 1995)] and MM5/SAQM [Pennsylvania State University–National Center for Atmospheric Research Mesoscale Model Version 5 (Grell et al. 1994) and San Joaquin Valley Air Quality Model (Chang et al. 1997)], in terms of their ability to reproduce the observed ozone air quality, and quantify the effects of changes in emissions on predicted ozone levels. To this end, we applied the U.S. Environmental Protection Agency's (EPA 1991, 1999) recommended statistical metrics, namely, unpaired accuracy, normalized bias, and normalized gross error, for evaluating photochemical grid models from the regulatory perspective. We also examined the effects of hypothetical reductions in the emissions of volatile organic compounds (VOC) and nitrogen oxides (NO_x) on ozone concentrations, to address the models' response to changes in emissions. We considered not only the level of improvement in predicted ozone but also the relative efficacies of VOC- and NO_x-focused controls.

In section 2, the meteorological conditions associated with three high-ozone events of the summer of 1995 in the eastern United States are discussed briefly. The meteorological, emissions, and air quality models used in this study are described in section 3. The ability of the two modeling systems to capture the salient features in ozone observations and the efficacies of hypothetical emission reduction options, namely, VOC-focused and NO_x-focused reductions, are examined in section 4. The key findings of this study are summarized in section 5.

2. Meteorological conditions

The formation and destruction of ozone in the planetary boundary layer (PBL) is governed by VOC and NO_x emissions and meteorological conditions. The meteorological aspects associated with high-ozone events in the northeastern United States were analyzed by Vukovich (1995), Ryan et al. (1998), Zhang et al. (1998), Berman et al. (1999), Zhang and Rao (1999), and Michelson and Seaman (2000). Briefly, a slow eastward-moving midtropospheric high pressure system over the United States is found to be the characteristic meteorological feature common to the three ozone events during the summer of 1995 (16–20 June, 12–16 July, and 30 July–2 August). The National Center for Environmental Prediction (NCEP) analyses of 500-mb geopotential height and winds over North America (not shown here), on the day preceding each episode, exhibit a cutoff low in the West Coast that reached low latitudes between 35° and 40°N, with a blocking high downstream during the following days. The 500-mb high pressure systems are usually accompanied by subsidence, clear skies, stronger shortwave radiation, high temperature, and a stagnant air mass near the ridge line of the sea level high pressure region. Another common synoptic-scale feature associated with high-ozone events in the eastern United States is the presence of a sea level subtropical high over the Atlantic Ocean, supporting low-level southwesterly winds in the coastal region that facilitate transport of pollutants from the southwest to the northeast. A sea level high pressure system over the U.S. continent, together with low pressure over Canada, provides a large meridional pressure gradient that supports westerly low-level jets, which is an important conveyor of pollutants from the Midwest to the Northeast during high-ozone days (STI 1999). The so-called Appalachian lee-side trough—a mesoscale low pressure system enhanced on the lee side of the Appalachian mountains—separates the subtropical high over the Atlantic Ocean from the continental high over land and enhances southwesterly winds along the urban corridor of the Atlantic coast (Pagnotti 1987).

3. Modeling systems

In this study, we applied two meteorological models (RAMS and MM5) and two Eulerian photochemical models (UAM-V and SAQM) using the same emissions inventory. While RAMS/UAM-V and

MM5/SAQM are treated as two separate modeling systems, it is possible to use any meteorological model's output with appropriate transformation techniques to drive a photochemical model (McNally et al. 1998; Biswas and Rao 2001). The MM5/SAQM system consists of the meteorological model MM5 (Grell et al. 1994), whose output is directly incorporated into the SAQM grid system (Chang et al. 1997). The RAMS/UAM-V system comprises the meteorological model RAMS (Pielke and Uliasz 1998), whose output is mapped onto the UAM-V grid system (Morris et al. 1992, 1993). These two modeling systems were applied to a geographical region that extends approximately from the middle of Kansas to the Atlantic coast, with the "data analysis grid" being limited to the area extending from 92° to 69.5°W and 32° to 44°N. Figure 1 displays the modeling domain for the RAMS/UAM-V system, the areal extent of the data analysis grid, and the definition of the three subregions.

a. Meteorological models

The salient features of the two meteorological models, RAMS and MM5, as applied in this study, are given in Table 1. To increase the compatibility between the two meteorological models, we used similar modeling domains consisting of two-way nests with 108 km × 36 km × 12 km horizontal grid dimensions. The vertical coordinates in both models are terrain-following, using a nondimensional height for RAMS and nondimensional pressure levels for MM5, extending up to 16 km. Also, both models adapt nonhydrostatic and primitive equations for the dynamics, include solar and terrestrial radiation, and use leapfrog and upstream advection schemes, time-splitting and vertical implicit schemes for the treatment of fast waves, nudging techniques for four-dimensional data assimilation (4DDA), and two-way nesting to facilitate interaction among domains. The major differences between the two meteorological models are in the treatment of the boundary layer processes and the lack of cloud condensation processes in RAMS (see Table 1). However, these high-ozone events are generally associated with clear-sky conditions and nonprecipitation periods and, thus, the lack of microphysical processes in RAMS should not be a major concern when modeling these ozone episodes. However, it should be noted that we used observed cloud cover and precipitation data in the UAM-V simulations, while for the SAQM simulations we used the variables derived from MM5. The setup of the two meteorological models is briefly described below.

The input data for RAMS were developed through a combination of the predicted pressure-level gridded data from the European Centre for Medium-Range Weather Forecasting (ECMWF), available every 6 h, and observations from the synoptic network covering the continental United States. Further details on the setup of RAMS and meteorological conditions during the three ozone episodes can be found in Kallos and Lagouvardos (1997). The input data for MM5 were the NCEP's global analysis fields along with the twice-daily upper-air soundings and 3-h surface observations. Further details on the MM5 setup can be found in Zhang and Rao (1999).

The meteorological outputs from RAMS and MM5 were preprocessed to provide inputs to the photochemical grid models; these meteorological fields are referred to as "model-ready" data. Hogrefe et al. (2001a,b) and Rao et al. (2000) compared the predicted and observed fields of temperature and wind speed, and found that both models were able to reproduce the observed spatial and temporal features on the synoptic and longer-term timescales but not on the intraday timescale (i.e., periods < 10 h). The model-ready layer 1 temperature distributions over the modeling domain for the morning (0600–1100 EST) and the afternoon (1200–1700 EST) periods averaged over the eight episode days for RAMS and MM5 are presented in Fig. 2 along with the measured data from about 330 stations in the domain. Although there are differences spatially, the observed temperature range of about 22°–

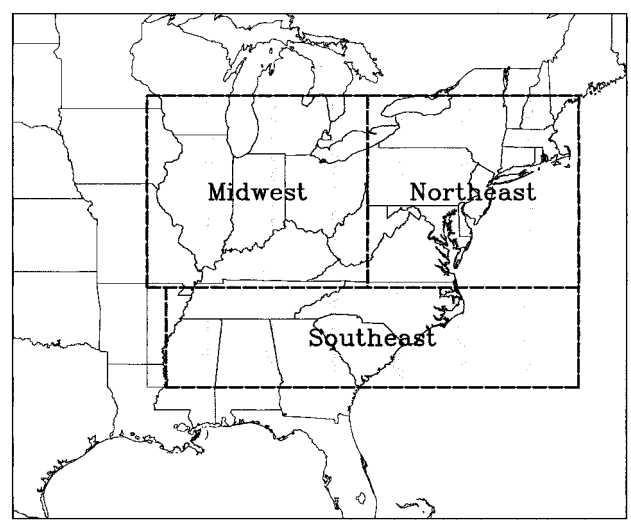

FIG. 1. Modeling domain for the RAMS/UAM-V system. The data analysis grid shown shaded is also the 12-km grid in the RAMS/UAM-V system. The three subregions over the analysis grid are identified as Northeast, Midwest, and Southeast for subregional analysis.

TABLE 1. Comparison between the RAMS3b and MM5 meteorological models as applied in this study.

Parameter	RAMS3b			MM5v1		
Grid size	108 km	36 km	12 km	108 km	36 km	12 km
Map projection	Rotational polar-stereographic			Lambert Conic Conformal (LCC)		
Center of D1	38.6°N, 91.3°W			40°N, 90°W		
Dimensions (x, y)	45 × 35	89 × 77	170 × 128	61 × 41	82 × 76	166 × 148
Grid	Arakawa C grid			Arakawa B grid		
Lateral boundary condition of D1	Nudging to ECMWF 6-hourly 4DDA output and 6-hourly surface observations			Nudging to enhanced mesoscale analyses using soundings and 3-hourly surface observations		
Nesting	Two-way			Two-way		
Upper boundary condition (UBC)	Solid wall with absorbing layer			Radiative UBC for all domains		
Vertical levels Below 850 mb Lowest level at	28 8 69 m	34 14 17 m	34 14 17 m	25 8 10 m	25 8 10 m	25 8 10 m
Air–land interaction	6-level soil model (–0.5–0 m)			Blackadar surface energy balance equation		
Vegetation and surface layer	Biosphere–Atmosphere Transfer Scheme (Dickinson et al. 1986; Louis 1979)			Blackadar (1979) 13 groups of surface physical parameters		
PBL	Mellor–Yamada TKE K theory for local closure			Nonlocal mixing in convective boundary layer (CBL) regime; K theory for non-CBL regimes		
Moist physics	moisture as a passive substance			Full microphysics with moisture, rain, clouds, ice, and water		
Clouds	No			High, middle, and low cloud coverage		
Cumulus Parameterization	No			Kuo scheme	Grell scheme	None
Shallow convection	No			Yes	Yes	Yes
Nudging coefficient (s^{-1}) 4DDA in PBl	$1.0\ 10^{-4}$ Yes			$2.0\ 10^{-4}$ Yes, but not for temperature and moisture		
Duration of simulations	1 Jun–31 Aug 1995			1 Jun–31 Aug 1995		

28°C has been captured by both models during the morning period. For example, both models exhibit similar spatial features of higher temperatures in the Midwest followed by a decrease over the Appalachian region and an increase toward the Atlantic coast, consistent with the measured data. However, during

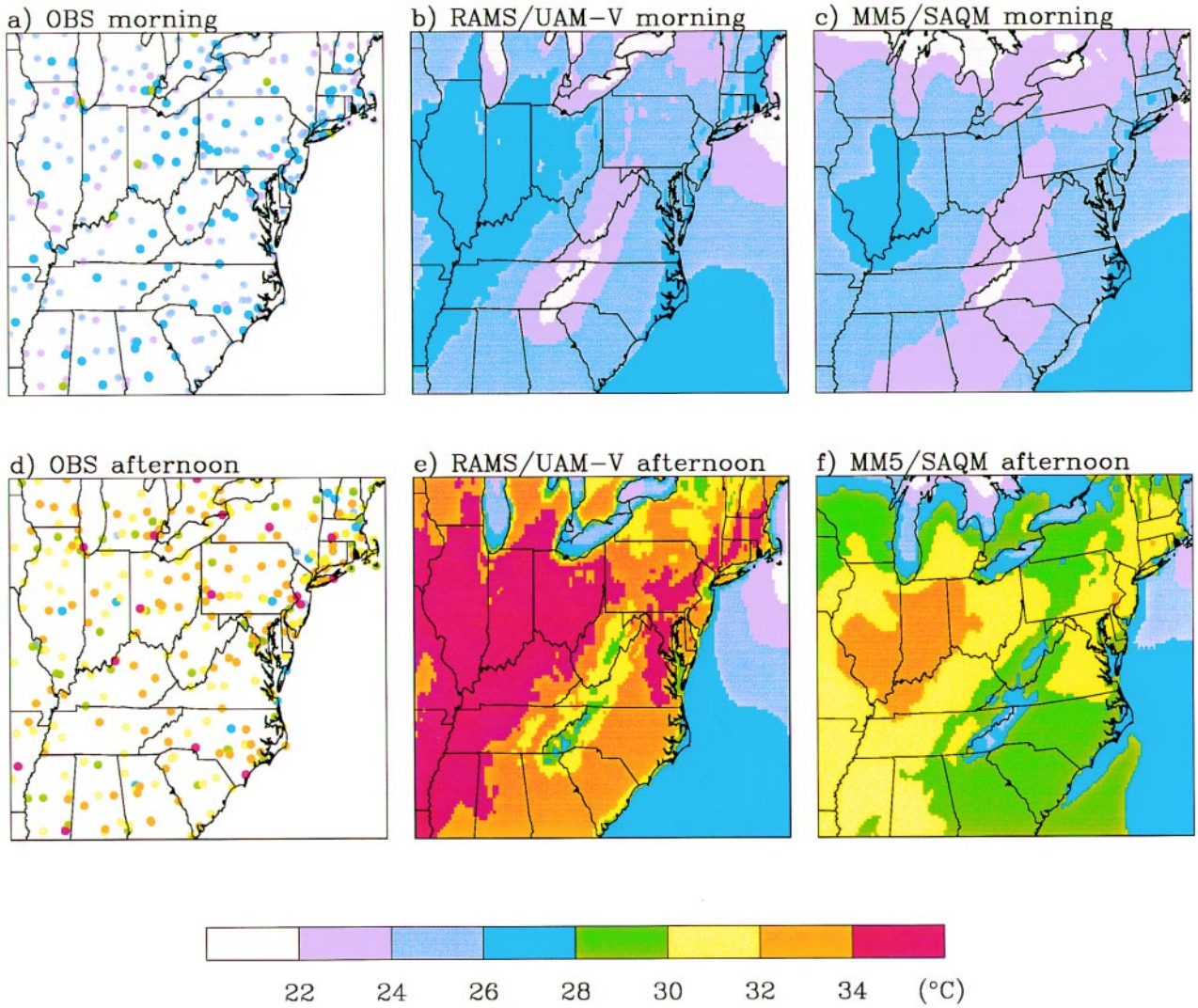

FIG. 2. [(a), (b), (c)] Layer 1 temperatures (°C) over the data analysis grid averaged over eight episode days during the morning (0600-1100 EST) period for the measured, RAMS/UAM-V, and MM5/SAQM, respectively. The measured averages are displayed as small dots, while the simulated values are color coded. [(d), (e), (f)] Layer 1 temperatures (°C) over the data analysis grid averaged over eight episode days during the afternoon (1200–1700 EST) period for the measured, RAMS/UAM-V, and MM5/SAQM, respectively. The measured averages are displayed as small dots, while the simulated values are color coded.

the afternoon period the RAMS-derived temperatures are generally higher than the measurements by about 2°–4°C, while those from MM5 are lower by about the same amount over some portions of the land. In contrast to the morning period, when both models have similar land–sea temperature gradients, RAMS exhibits a much sharper gradient than MM5 during the afternoon period.

The average layer 1 wind speeds are displayed in Fig. 3 for both models, as well as measured data for the morning and afternoon periods. During the morning period, both models exhibit a similar spatial pattern with winds in the 2–3 m s^{-1} range over the central portions of the domain, increasing gradually toward the coastal region. This feature appears to agree with the measured data (see Figs. 3a–c). Although both models exhibit a similar spatial pattern for the afternoon period, the model-derived wind speeds are generally lower than measured data, mainly in the central portions of the domain (see Figs. 3d–f). The differences in the temperature and wind speed between these two models are attributable to the differences in the analysis fields, boundary conditions, and physical processes considered (see Table 1). Thus, these simulations with RAMS and MM5 should be viewed as one of several plausible outcomes given the differences in the input data and methods employed for data assimilation.

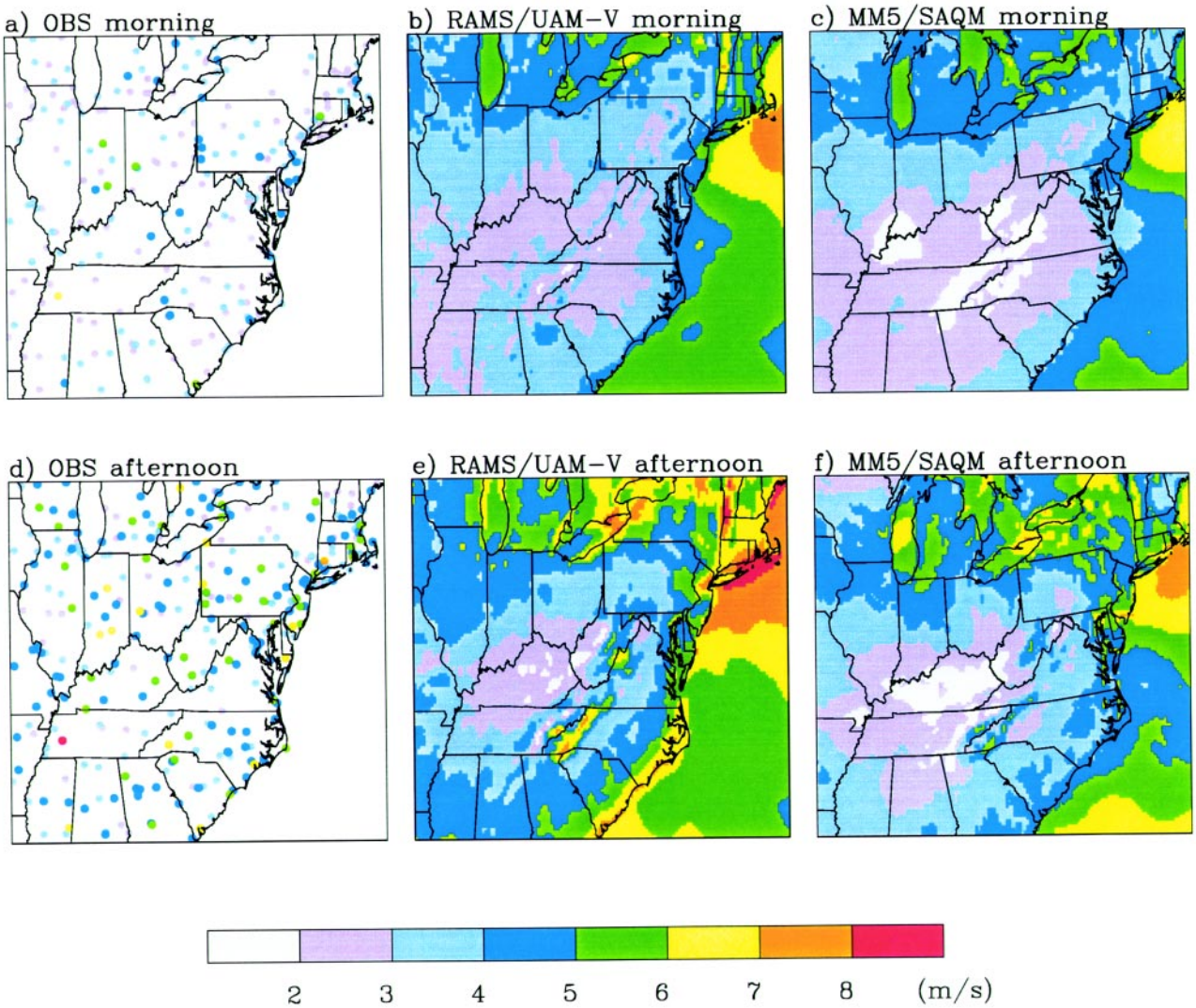

FIG. 3. [(a), (b), (c)] Layer 1 wind speeds (m s^{-1}) over the data analysis grid averaged over eight episode days during the morning (0600–1100 EST) period for the measured, RAMS/UAM-V, and MM5/SAQM, respectively. The measured averages are displayed as small dots, while the simulated values are color coded. [(d), (e), (f)] Layer 1 wind speeds (m s^{-1}) over the data analysis grid averaged over eight episode days during the afternoon (1200–1700 EST) period for the measured, RAMS/UAM-V, and MM5/SAQM, respectively. The measured averages are displayed as small dots, while the simulated values are color coded.

b. Emissions model

The initial emissions database was adopted from OTAG (EPA 1997), which was originally developed for the July 1995 ozone episode. These emissions were updated and processed with the Emissions Modeling System (EMS95 model; M. Janssen 1998, personal communication), to generate gridded inputs to the photochemical model. Contributors to anthropogenic emissions include point, area, and mobile source categories, which are described below.

1) POINT SOURCES

The OTAG database for some of these sources was updated by E. H. Pechan and D. Solomon (1998, personal communication) by correcting stack parameters and emissions. Monthly fuel-use data for June, July, and August 1995 were obtained for some of the electric utility facilities from the published reports of the U.S. Department of Energy (USDOE) and the acid rain database. In the OTAG work, the electric utility sector emissions were estimated on the basis of fuel consumption for the month of July. Following this approach, the fuel-use data for June and August were compiled from USDOE and acid rain databases for those facilities that could be matched with the OTAG inventory. Emissions for June and August were estimated by appropriately prorating the fuel-use data for these two months based on fuel-use and emissions data

for July. These data were then processed with EMS95 for use in photochemical models. Based upon July 1995 emissions data, 300 individual point sources and 30 collocated sources were identified for the plume-in-grid (PiG) option for use in UAM-V. It should be noted that SAQM does not have the PiG option.

2) Area and mobile sources

Any errors and omissions in the OTAG inventory for area sources were corrected, and emissions were processed with the EMS95 model (M. Janssen 1998, personal communication). Since mobile source emissions are temperature-dependent, emissions data for the modeling domain were processed with the EMS95 model using the UAM-V layer 1 temperature data.

3) Total emissions

Biogenic emissions over the modeling domain were estimated using the UAM-V layer 1 temperature and observed cloud cover with the Biogenic Emissions Inventory System 2 (BEIS2) model (Guenther et al. 1993; Geron et al. 1994). In the surface layer, about 85% of the total VOCs are due to biogenic sources, and about 53% of the total NO_x emissions are from area and mobile sources. The surface-level carbon monoxide emissions constitute about 93% of the total emissions, with elevated sources contributing the rest. The day-to-day variation in the emissions of the biogenic and ground-level anthropogenic sources reflect the variations in the temperature and changes in activity levels, while elevated emissions are fairly uniform over these episode days. These emission data were also used in the MM5/SAQM simulations.

c. Photochemical models

The key features of the two Eulerian photochemical models, UAM-V and SAQM, and their setup in this study are summarized in Table 2. The two modeling systems are briefly described below.

1) RAMS/UAM-V modeling system

The RAMS/UAM-V modeling system consists of the UAM-V, Eulerian photochemical model version 1.24 using the Carbon Bond 4 (CB4) mechanism (Gery et al. 1989) with a fast chemistry solver and updated isoprene chemistry (Deuel et al. 1996), and meteorological data from RAMS. Details on the UAM-V model can be found in Scheffe and Morris (1993) and information on updated isoprene chemistry is available on the OTAG Web site (OTAG 1997). This model has been applied previously in the development of emission controls strategies for mitigation of the ozone problem (OTAG 1997). The UAM-V modeling domain consists of a horizontal two-way nested grid at 36 and 12 km, corresponding to 64 × 63 cells and 137 × 110 cells, respectively (see Fig. 1). The UAM-V domain in the vertical extends up to 4 km above the surface and consists of 14 levels, with layer 1 set at 50 m.

Initial and boundary conditions

The initial and boundary conditions for the precursor concentrations in UAM-V were set at the tropospheric background levels and the model was allowed to spin up for three days preceding each episode with pertinent emissions and meteorological conditions. Ozone concentrations along the boundary of the model domain were specified based on the available ground-level ozone observations from stations located near the boundaries and from ozonesonde observations taken at Boulder, Colorado; Goosebay and Churchill, Canada; and Bermuda.

2) MM5/SAQM modeling system

The MM5/SAQM system consists of the meteorological model MM5 (Grell et al. 1994), meteorological and emissions preprocessors, and the SAQM (Chang et al. 1997), which is an Eulerian photochemical air quality model. Unlike UAM-V, which in this study utilizes two-way nested 36- and 12-km domains, the SAQM has been applied to the 12-km domain. SAQM also uses the CB4 chemical mechanism, which was updated with the new isoprene chemistry developed by Carter (1996). The SAQM's grid structure follows essentially that of MM5 and is in the LCC projection system. The SAQM domain consists of 161 cells along east–west and 143 cells along north–south. There are 16 layers in the vertical direction up to 8715 m above the surface, with layer 1 set at 10 m.

Initial and boundary conditions

Since the SAQM version used in this study cannot accept time-dependent boundary conditions based on observations, an iterative method was used to generate the boundary conditions for the SAQM simulations for all episodes. The model is initialized with background concentrations of chemical species and is simulated for a period of 48 h, with the corresponding meteorology and emissions to obtain the initial conditions. The boundary conditions reflect the last hour of the previous day's results.

3) Emissions

Both RAMS/UAM-V and MM5/SAQM utilized the same emissions database. Using appropriate coor-

TABLE 2. Comparison between the setup of the two photochemical grid models, UAM-V and SAQM.

Parameter	UAM-V	SAQM
Meteorological input	RAMS3b results interpolated horizontally and vertically into lat/long grid by RAMS2UAM converter. Observed precipitation and cloud cover information is used.	MM5v1 results extracted by San Joaquin Valley meteorological preprocessor (SMPP) Diagnosed precipitation and cloud cover from MM5 results are used
Emission inputs	Prepared by EMS95	Interpolated the gridded emission used by UAM-V and processed by EPS preprocessor
Vertical structure	14 layers from surface to 4 km. First layer is 50 m thick. 10 layers in the lowest 1.5 km.	16 layers from surface to 8.7 km. First layer is centered at 10-m level. 8 layers in the lowest 1.5 km.
Horizontal structure	lat/long coordinates. 36-km coarse grid (64 × 63 cells) nested with 12-km analysis grid (137 × 110 cells).	LCC 12-km grid (161 × 143 cells)
Initial condition	Background values applied at 0000 EST of 1 Jun 1995	Background values applied at the beginning of the three episodic runs and then going through iterative initialization process
Boundary condition	Ozone values interpolated from surface observations and ozonesondes, varying temporally and spatially. Other species are in background values.	From last hour of previous day's results, fixed temporally.
Simulation period	Running continuously from 1 Jun to 31 Aug 1995. 8 days selected in the analysis are part of the seasonal simulation.	Three episodic runs started at 1200 UTC 16 Jun, ended at 0000 UTC 21 Jun; started at 1200 UTC 10 Jul ended at 0000 UTC 16 Jul; started at 1200 UTC 30 Jul, ended at 0000 UTC 3 Aug.
Chemistry	CB4 mechanism with new isoprene chemistry	CB4 mechanism with new isoprene chemistry
Chemistry solver	Systems Application International's (SAI) fast solver (SAI 1995)	Standard quasi–steady-state approximation solver
Horizontal advection	Smolarkiewicz's scheme	Bott's scheme
Vertical mixing	K-theory	Blackadar (1979) nonlocal closure for convective condition; K-theory for others
Plume-in-grid	300 top ranking NO_x elevated point sources were selected for plume-in-grid treatment.	Option is not available.

dinate transformation from the latitude–longitude for the LCC projection system and the UAM-V–ready surface-level emissions were mapped into the SAQM domain. For point sources, the latitude–longitude locations were converted into the LCC system, and the emissions were reassigned to the appropriate elevated

layer of the modeling domain based upon the effective plume height of the point source.

4. Results and discussion

In the following, we examine the models' ability to reproduce the observed ozone concentrations at individual monitoring stations as well as the spatial and temporal variations for three high-ozone events that occurred in the summer of 1995. In addition, the models' response in terms of changes in ozone levels and directionality for emission controls (i.e., NO_x and VOC reductions) is examined using hypothetical reductions in precursor emissions.

a. Model performance evaluation

All applications of photochemical modeling systems in a regulatory setting require that their performance in reproducing the observed ozone air quality be evaluated by comparing the model-predicted pollutant concentrations with measurements using a set of statistical measures (EPA 1991, 1999). In this study, we compare the daily maximum measured and predicted ozone concentrations at the monitoring stations for the eight episode days, recognizing the limitation that observations reflect point measurements, while model predictions represent volume-average concentrations.

1) Spatial patterns of daily maximum ozone

As a first step in model evaluation, we compare the spatial patterns of predicted daily maxima at each grid cell with the measured daily maxima over the analysis domain. As an illustration, Fig. 4 displays 1-h ozone maxima for three out of the eight episode days simulated in this study. Since our aim here is to examine whether the modeling systems are able to reproduce the spatial pattern in the observed ozone concentrations, the modeled daily ozone maxima are

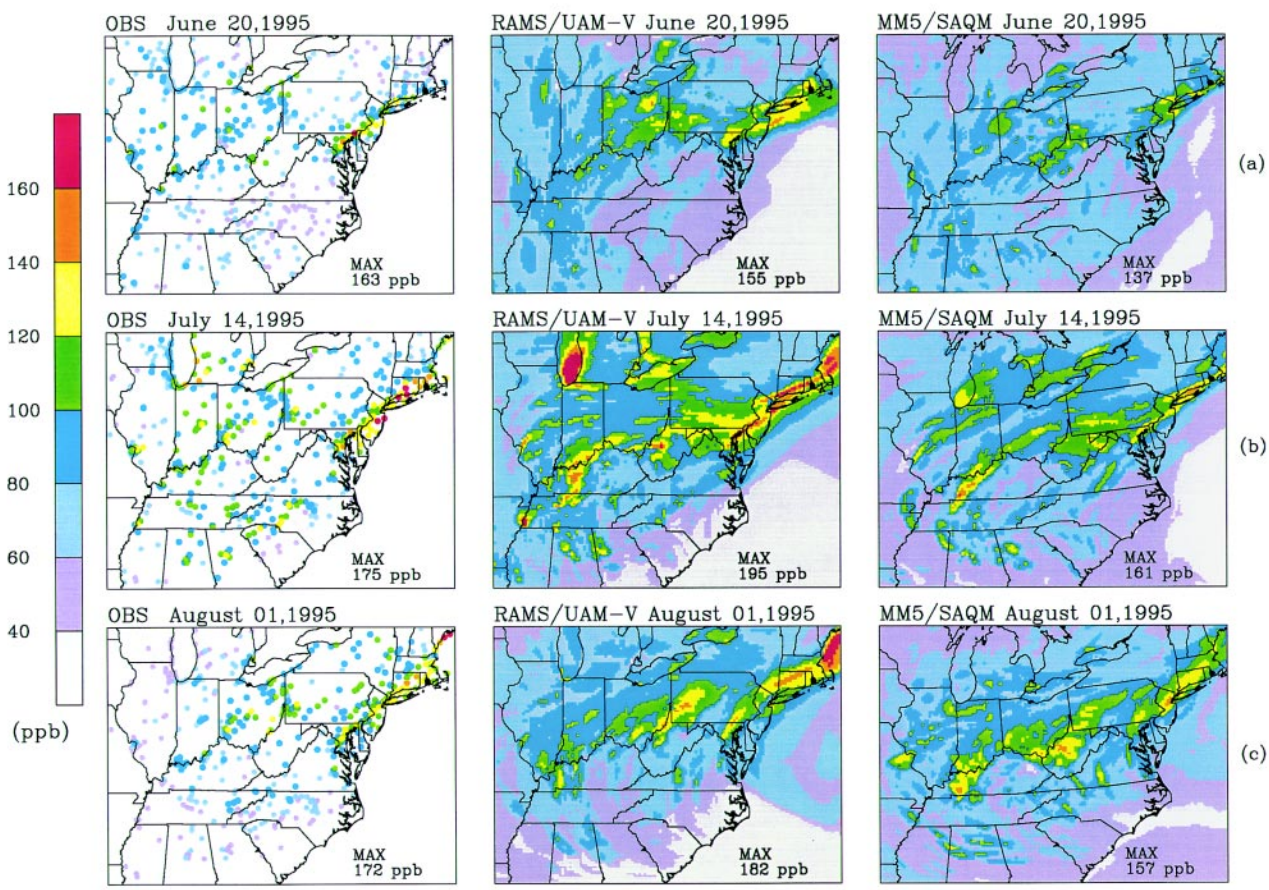

Fig. 4. Measured (left), and simulated [(middle), (right)] of daily maximum 1-h ozone concentrations (ppb) for (top) 20 Jun, (middle) 14 Jul, and (lower) 1 Aug 1995 over the analysis domain. The observed maximum concentrations (shown as small dots) are at the monitoring stations for the episode day, and model predicted represents the daily 1-h ozone maxima at each grid cell for the same day. The maximum ozone concentrations over the whole domain are shown in the right-hand corner of each panel.

shown at all grid cells instead of at each monitoring location.

(i) The 19–20 June 1995 episode

The observed 1-h ozone maxima along the northeastern urban corridor region are 157 and 163 ppb on 19 and 20 June, respectively. The 1-h ozone maxima predicted by RAMS/UAM-V and MM5/SAQM in the northeastern urban corridor region are 140 and 155 ppb, and 126 and 137 ppb for 19 and 20 June, respectively. The measured daily maxima at each monitoring station and the predicted grid-cell maximum for 20 June 1995 for the two modeling systems are displayed in Fig. 4a. The measured maximum ozone levels are generally less than 100 ppb over major portions of the domain, with the exception of the northeastern urban corridor where ozone levels are above 120 ppb at several monitoring locations, a feature captured by both models. However, the simulations of the two models differ over large areas of the Midwest and Southeast in terms of spatial gradients and absolute concentration levels.

(ii) The 13–15 July 1995 episode

During this period, many locations over the eastern United States reported ozone maxima well above the level of the 1-h ozone standard. The measured maxima over the analysis grid are 178, 175, and 184 ppb on 13, 14, and 15 July, respectively. Figure 4b displays the measured maximum ozone concentration at each monitoring station and the model-predicted ozone maximum at each grid cell for the two models for 14 July. Once again, the measured high ozone levels are generally confined to the northeastern urban corridor and a few locations along the eastern Lake Michigan region. These broad patterns of the observed maximum ozone are captured well by both modeling systems. However, the pattern of high ozone predicted by the two modeling systems over Tennessee and Kentucky is not evident in the observations.

(iii) The 31 July–2 August 1995 episode

The August 1995 episode is characterized by ozone maxima of 172 and 150 ppb on 1 and 2 August, respectively, occurring over coastal Maine. Figure 4c displays the measured maximum ozone and model-predicted daily maximum ozone concentrations for 1 August 1995. Both models predicted high ozone levels along portions of the northeastern corridor that extends from New York/New Jersey into Maine, consistent with observations. However, the maximum ozone predicted over the Pennsylvania/West Virginia region is not evident in observations. It should be noted that, while there is a general agreement between the measured and predicted spatial distribution patterns of ozone maxima, there are localized differences between observations and predictions in the two modeling systems. Since the emissions inventory database and the chemical mechanism are common to both modeling systems, these differences reflect the differences in the adopted meteorological fields as well as differences between the design of the two photochemical models as noted in Table 2.

2) Diurnal variation

A comparison is made between the observed and predicted hourly ozone concentrations for selected periods of the diurnal cycle. Following Tesche et al. (1990), the predicted values are interpolated to the monitor location using the four nearest grid cells surrounding the monitor. The four time periods considered are 0600–1000, 1000–1400, 1400–1800, and 1800–2200 EST. Briefly, these four periods can be characterized as follows. During the 0600–1000 EST period there is injection of fresh emissions in the surface layer, and the mixing layer starts to grow rapidly. The 1000–1400 EST period reflects the time during which photochemical reactions, vertical mixing, and advection processes dominate. During the 1400–1800 EST period, the mixed layer starts to collapse with decreasing solar insolation. The 1800–2200 EST period is characterized by the dominance of nighttime chemical and removal processes. It should be noted that the relative roles of different atmospheric processes are not constrained to these specific time periods since they can overlap; these periods are considered here for examining the overall temporal response of the modeling systems in relation to the observed data.

At each monitoring station for each one of these selected periods, the difference in ozone concentrations at the beginning and ending hour (i.e., the ozone tendency) was obtained for each of the eight episode days, and the average concentration for the period is computed for the observed and the predicted values. Figures 5a–f are scatterplots of these differences in observed and predicted ozone concentrations for the two models for each of the time periods. Also listed are the mean, standard deviation, and the correlation coefficient between the observed and predicted tendencies based on 489 monitors or data points for each time period.

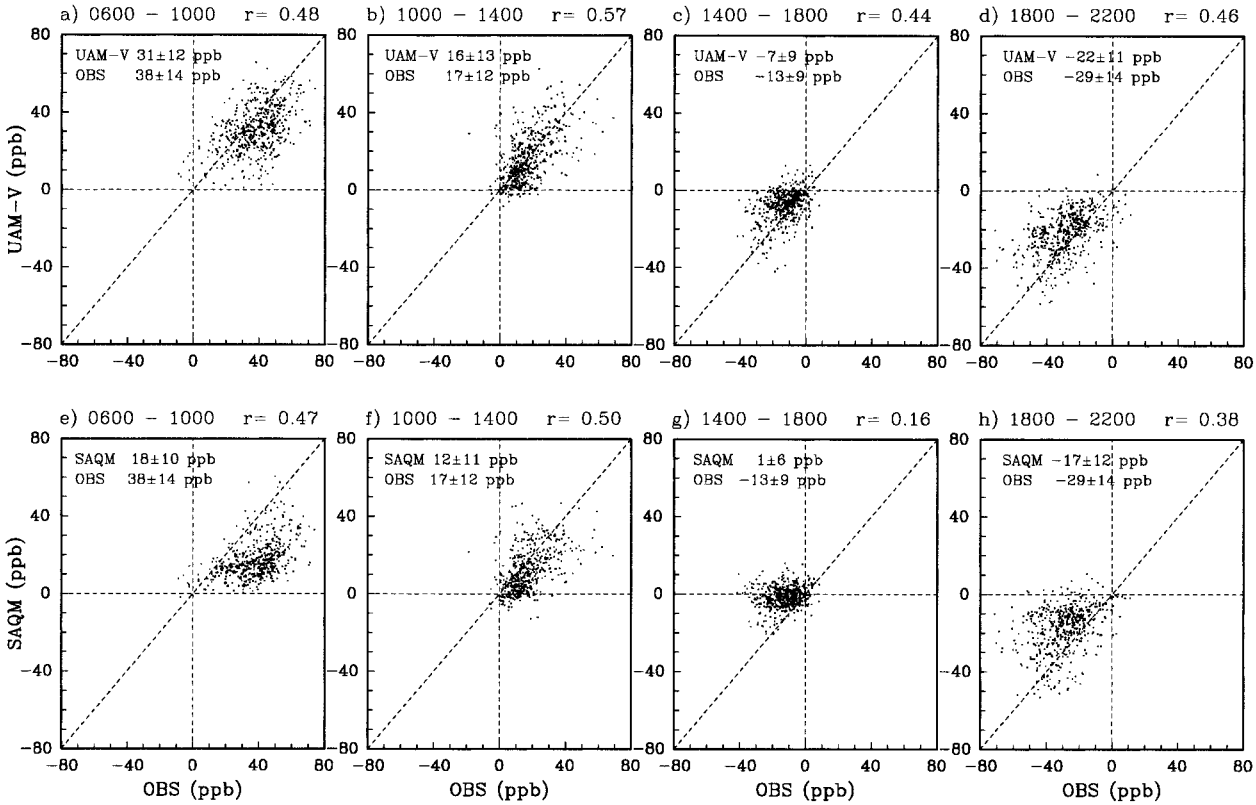

FIG. 5. For each of the selected time periods the ozone difference (ppb) is the difference in the hourly ozone concentrations at the beginning and ending hour. Scatterplots depict the observed and predicted ozone differences averaged over the eight episode days for selected time periods, (a) 0600–1000, (b) 1000–1400, (c) 1400–1800, and (d) 1800–2200 EST at all monitoring locations over the analysis grid for RAMS/UAM-V and (e)–(h) are for MM5/SAQM for the same time periods. The 1-to-1 line and the zero concentration difference are shown as dotted lines. Also listed for each of the above time periods are the average and standard deviation of the measured and predicted ozone concentration differences, and the correlation coefficient (r) between observed and predicted differences.

For the 0600–1000 EST period, the correlation coefficients between the measured and predicted values are very similar for both modeling systems. However, a visual examination of the scatterplots reveals bias in SAQM when compared with UAM-V (see Figs. 5a,f). This is also evident from the comparison of the mean ozone difference of 38 ppb from observations to the 31 and 18 ppb predicted by UAM-V and SAQM, respectively. For the 1000–1400 EST period, which is associated with increased photochemical activity and vertical mixing, the UAM-V predicted average ozone difference is in better agreement with the observations than SAQM. During 1400–1800 EST, when the photochemical activity begins to decrease and the mixed-layer height starts to fall along with reduced solar insolation, SAQM shows a poor relationship to the observed ozone differences when compared to UAM-V. The scatterplots, Figs. 5c and 5g, indicate that a majority of the SAQM predictions are off the zero difference line. This is also borne by the average ozone differences of 1 and –7 ppb for SAQM and UAM-V, respectively, compared to the –13 ppb based on observations. During the 1800–2200 EST period, there is some improvement in the scatter between the models and measured data (see Figs. 5d,g). However, there appears to be no improvement in the predicted average ozone differences of –17 ppb for SAQM and –22 ppb for UAM-V versus –29 ppb in the observed data, again suggesting the presence of bias in the case of SAQM. The largest measured average ozone differences are found to occur in the morning (0600–1000 EST) and the evening (1800–2200 EST) periods, a feature that is captured qualitatively by both modeling systems. Thus, these results indicate that the observed range of differences in ozone concentrations has been more successfully captured by RAMS/UAM-V than by MM5/SAQM.

To examine if there are spatial differences between the predicted and measured ozone diurnal cycles, we compared the amplitude and phase shift for the diur-

nal oscillation over the three subregions identified as Northeast, Midwest, and Southeast in Fig. 1. The amplitude is defined as the difference between the maximum and minimum hourly ozone concentrations for the day. A histogram plot of the differences between the predicted and observed amplitudes of the diurnal concentration is presented in Fig. 6 with urban (shown as unfilled bars) and nonurban (shown as filled bars) monitoring locations for the analysis grid and the three subregions. In this study, a monitoring station is defined as urban if it is located in a grid cell whose urban land-use classification is 70% or higher. These plots show that at a majority of nonurban locations, both modeling systems underpredicted the amplitude of the diurnal oscillation, with SAQM's underestimation more pronounced than UAM-V. In an ideal simulation, the differences between the predicted and observed amplitudes would be zero. Figure 6 exhibits a distribution of the differences extending beyond ±40-ppb range. In the case of the nonurban monitors (filled bars), SAQM exhibits a skewed distribution for all three subregions with a large segment of the sample underpredicting, whereas the distributions for UAM-V appear symmetric. The urban monitors (unfilled bars), on the other hand, exhibit a less-skewed distribution in the case of SAQM, while the distribution is symmetric for UAM-V with the exception of the Southeast subregion. This suggests that on a geographical basis both models do poorly in capturing the observed diurnal ozone amplitude in the Southeast subregion compared to the other areas of the analysis domain.

Defining phase shift as the difference between the observed and modeled time of occurrence of the daily 1-h ozone maximum, Fig. 7 displays the phase differences at urban and nonurban monitoring locations for the three subregions. Both the Northeast and Midwest subregions exhibit the predicted peak occurring about

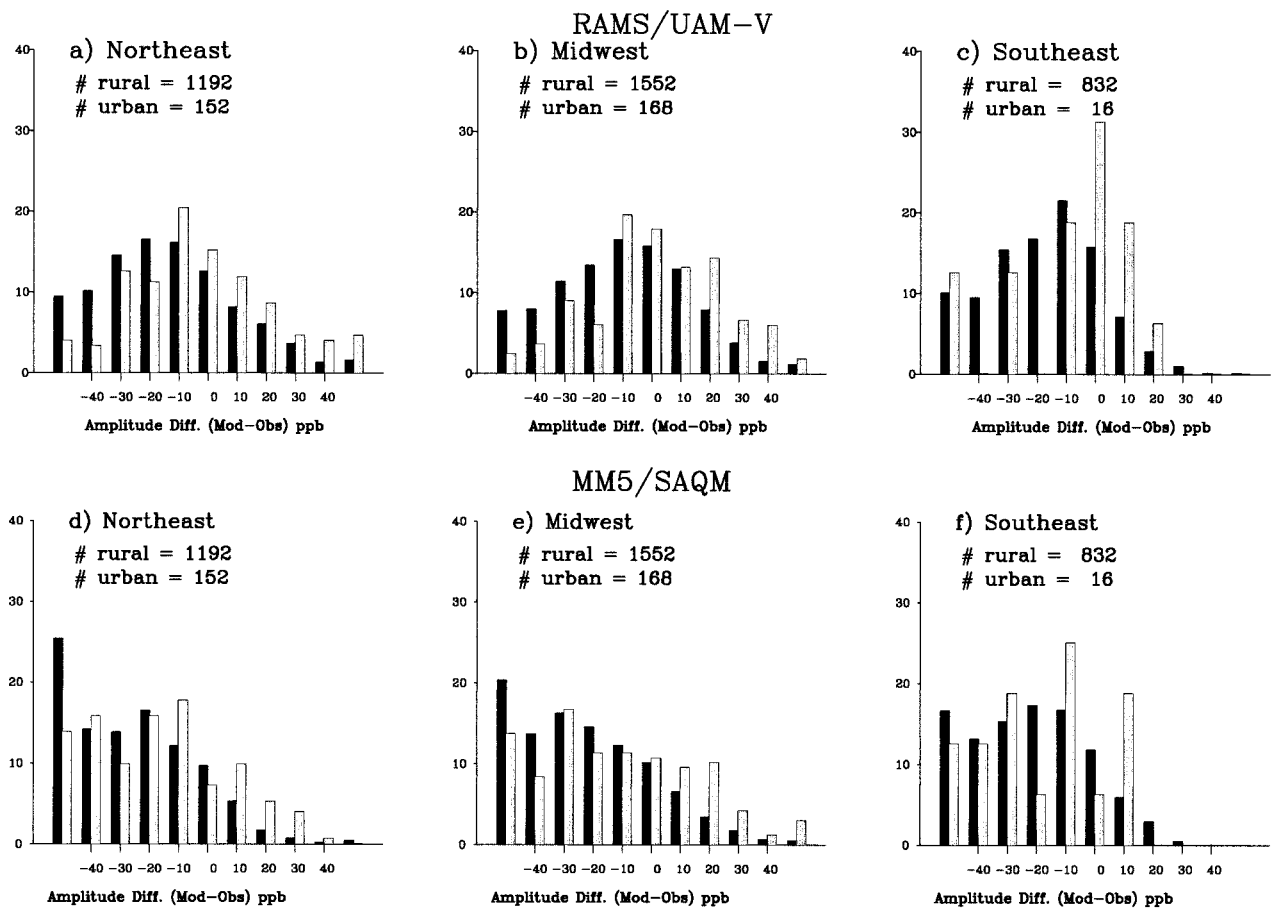

FIG. 6. Histogram plot, expressed as a percent of the number of monitoring stations [urban (unfilled) and nonurban (filled)], for the eight episode days over the three subregions—[(a), (d)] Northeast, [(b), (e)] Midwest, and [(c), (f)] Southeast for RAMS/UAM-V and MM5/SAQM. The abscissa (ppb) is the difference between model amplitude and the observed amplitude at a monitoring station, with amplitude defined as the difference between the daily maximum and minimum ozone concentration. Also listed in each panel are the number of data points (urban and rural) for each subregion.

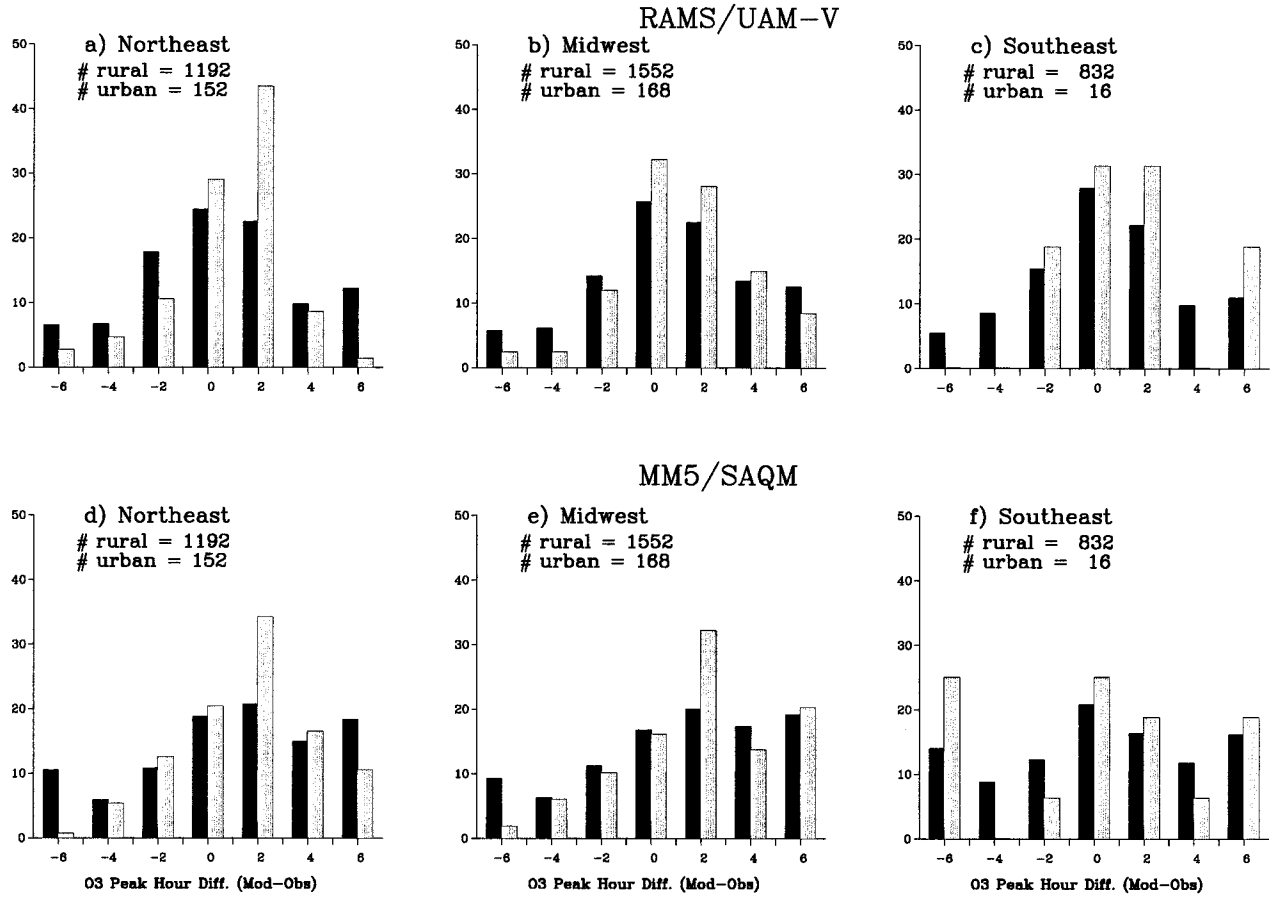

FIG. 7. Histogram plot, expressed as a percent of the number of monitoring stations [urban (unfilled) and nonurban (filled)], for the eight episode days over the three subregions—[(a), (d)] Northeast, [(b), (e)] Midwest, and [(c), (f)] Southeast for RAMS/UAM-V and MM5/SAQM. The abscissa (h) is the difference or lag between the hour of occurrence of the predicted and observed daily ozone maximum. Also listed in each panel are the number of data points (urban and rural) for each subregion.

2 h after the measured peak, both for urban and rural monitors for the two modeling systems. However, in the case of the Southeast subregion, both models differ in terms of their distributions for both urban and rural monitors, even though the UAM-V distributions are much more in line with the other two subregions. This conclusion is similar to that noted before, in that on a geographical basis the predictions for the Southeast subregion differ from the other areas of the analysis domain.

3) STATISTICAL MEASURES OF MODEL PERFORMANCE

Tesche et al. (1990) and the EPA (1991) recommended several statistical measures to perform operational evaluation of the grid-based urban-scale photochemical models. Sistla et al. (1995), Hanna et al. (1996), Tesche and McNally (1997), and Lurmann and Kumar (1997) have applied some of these measures in the evaluation of urban and regional-scale photochemical models. In this study, we applied a total of four statistical measures, the first three of which have been recommended by the EPA to assess model performance; these are (i) unpaired accuracy, (ii) normalized bias, (iii) normalized absolute gross error, and (iv) correlation coefficient, as defined in Table 3. The database used in this analysis consists of the predicted and measured daily maximum 1-h ozone concentrations at all monitoring stations for each episode day, and, as such, these data are paired in space but not necessarily in time. In other words, for each episode day there is one set of measured and predicted maximum ozone, providing a total of eight pairs for the eight episode days at each one of the 489 monitoring stations in the data analysis grid. The statistical metrics have been calculated for the analysis grid as well as the three subregions (see Fig. 1), and the results are summarized in Table 3.

(i) Unpaired accuracy (%)

This statistical measure compares the accuracy of the maximum measured and predicted ozone concen-

TABLE 3. Summary of statistical measures for the analysis grid, and the three subregions (Northeast, Midwest, and Southeast) for the eight episode days for UAM-V and SAQM.

Parameter	Analysis grid		Northeast		Midwest		Southeast	
	UAM-V	SAQM	UAM-V	SAQM	UAM-V	SAQM	UAM-V	SAQM
Sample size	3912		1344		1720		848	
Unpaired accuracy (%)[a]	–4	–11	–4	–11	–8	–22	–9	–5
Normalized bias (%)[b]	6	8	–1	0	14	10	3	15
Normalized gross error (%)[c]	20	23	20	28	20	24	22	25
Correlation[d]	0.66	0.52	0.66	0.52	0.49	0.30	0.70	0.51

[a]Unpaired Accuracy: $\frac{P_{\max} - O_{\max}}{O_{\max}}$,

where P_{max} and O_{max} are the maximum predicted and observed values, respectively, of all the stations.

[b]Normalized Bias: $\frac{1}{N}\sum_{i=1}^{N}\frac{P_i - O_i}{O_i}$,

where, P_i and O_i are the predicted and observed values, respectively, at station i, and N is the total number of stations.

[c]Normalized Average Absolute Gross Error: $\frac{1}{N}\sum_{i=1}^{N}\frac{|P_i - O_i|}{O_i}$.

[d]Correlation Coefficient: $\frac{\sum_{i=1}(P_i - \overline{P})(O_i - \overline{O})}{\sqrt{\sum^{N}(P_i - \overline{P})^2}\sqrt{\sum^{N}(O_i - \overline{O})^2}}$,

where P and O are the mean predicted and observed values, respectively, of all stations.

trations unpaired in time or in space. It should be noted that this statistical measure may not be very meaningful given the large areal extent of the modeling domain. However, it was included in this study since it is one of the recommended metrics in the regulatory analysis (EPA 1991). For the eight episode days considered in this study, this statistic varied from 1% to –19% for UAM-V and 3% to –24% for SAQM, while the EPA-recommended range is ±15%–20% for an acceptable model performance. Considering all episode days as one group, the unpaired accuracy estimates are –4% and –11% for UAM-V and SAQM, respectively, which is well within the range of the acceptance criteria. However, the metric for the three subregions shows that the Midwest subregion would not pass the criteria for SAQM, while both models have met the criteria for the other two subregions.

(ii) Normalized bias (%)

This statistic provides for an estimate of the bias in the models. The EPA (1991) recommends a range of ±5%–15% for this statistic as an acceptable level of model performance. For the eight episode days, this statistic ranges from –4% to 30% for UAM-V and –8% to 35% for SAQM, indicating that only some of the episode days would meet the criteria of acceptable

model performance. However, when all episode days are considered, the normalized bias is 6% and 8% for UAM-V and SAQM, respectively, which is well within the EPA's criteria for acceptable model performance. On a geographical basis, the three subregions also meet the criteria for both models.

(iii) Normalized absolute gross error (%)

This metric reflects an overall bias between predicted and measured ozone concentrations in contrast to the normalized bias in which the over- or underpredictions could cancel each other out. The EPA (1991) suggested a range of 30%–35% as an acceptable level of model performance for this metric. In this study, the metric for the eight episode days varied from 16–23% in the case of UAM-V and 20%–29% for SAQM, well within the criteria for acceptable model performance. Grouping all episode days, the estimated errors are 20% and 23% for UAM-V and SAQM, respectively, which are well within the acceptable level of model performance. Also, the metrics for the three subregions are within the level recommended for model acceptance.

(iv) Correlation coefficient

This statistic, although not explicitly recommended, has often been applied in earlier model evaluation studies. The day-to-day estimates of correlation varied from 0.50 to 0.76 for UAM-V and from 0.47 to 0.65 for SAQM, indicating a similar level of performance by both models. With all episode days grouped, the correlation for UAM-V is 0.66 and is 0.52 for SAQM. Geographically, the Midwest subregion has lower correlation for both models compared to the other two subregions.

In addition, application of other statistical metrics cited in Tesche et al. (1990) indicate that, while the performance of the two models differed on individual days, these differences are reduced considerably when model predictions are considered as an ensemble of all days simulated.

b. Ozone response to emission reductions

Even if there was perfect agreement between the simulated and observed ozone concentrations, the question that is of most interest to policy makers is "do the two modeling systems predict a similar response to difference emissions reduction options?" To examine this policy-relevant issue, we simulated two emission reduction scenarios using "across-the-board," or uniform, reductions in NO_x and VOC emissions amounting to 25% NO_x and 50% VOC (the VOC-focused reduction scenario labeled as N25V50 in Fig. 8), and 50% NO_x and 25% VOC (the NO_x-focused reduction scenario labeled as N50V25 in Fig. 8). In these two simulations, the initial/boundary conditions, meteorological fields, and biogenic emissions in the domain remained unchanged from the base case (labeled as N00V00, reflecting no emissions reductions). To assess the response of the emission reductions, a metric—the index of improvement—is defined as:

$$\text{Index of improvement (\%)} = \frac{(O_3)_{\text{base}} - (O_3)_{\text{control}}}{(O_3)_{\text{base}}} \times 100\%$$

where O_3 is the 1-h daily maximum ozone concentration at each grid cell.

The index of improvement at each grid cell of the analysis domain is averaged over the eight episode days for the two emission reduction scenarios and displayed in Fig. 8. The VOC-focused scenario (N25V50) reveals localized differences in the index of improvement between the two modeling systems (see Figs. 8a,b). While the index of improvement varies from no improvement to 15% in both models, the UAM-V predicts greater than 5% improvement over SAQM in a large portion of the analysis domain. Also, the few areas exhibiting no change are not necessarily the same geographical regions between the two models. In contrast to the VOC-focused scenario, the differences between the two models are most pronounced for the NO_x-focused scenario (see Figs. 8c,d). The urban areas of New York City, Chicago, and their surroundings, as well as other major population centers, have an improvement of 5% to 10%, with the exception of a few pockets, with most of the rural areas indicating an improvement in the range of about 15%–25%. The highest level of improvement, 25%–30%, is predicted by SAQM over portions of Tennessee and North Carolina, while the response of UAM-V in that region is in the 15%–25% range. Similar ranges of differences are evident between the two models in portions of Illinois and Wisconsin.

An examination of the coefficient of variation (CV), which is defined as the ratio of the standard deviation to the average, provides a means to assess day-to-day variability in the index of improvement over the analysis domain. Figures 9a–d display the spatial distribution of the CV for the two scenarios for the two models for the three episodes. In general, the higher variability of 70% or more is associated with

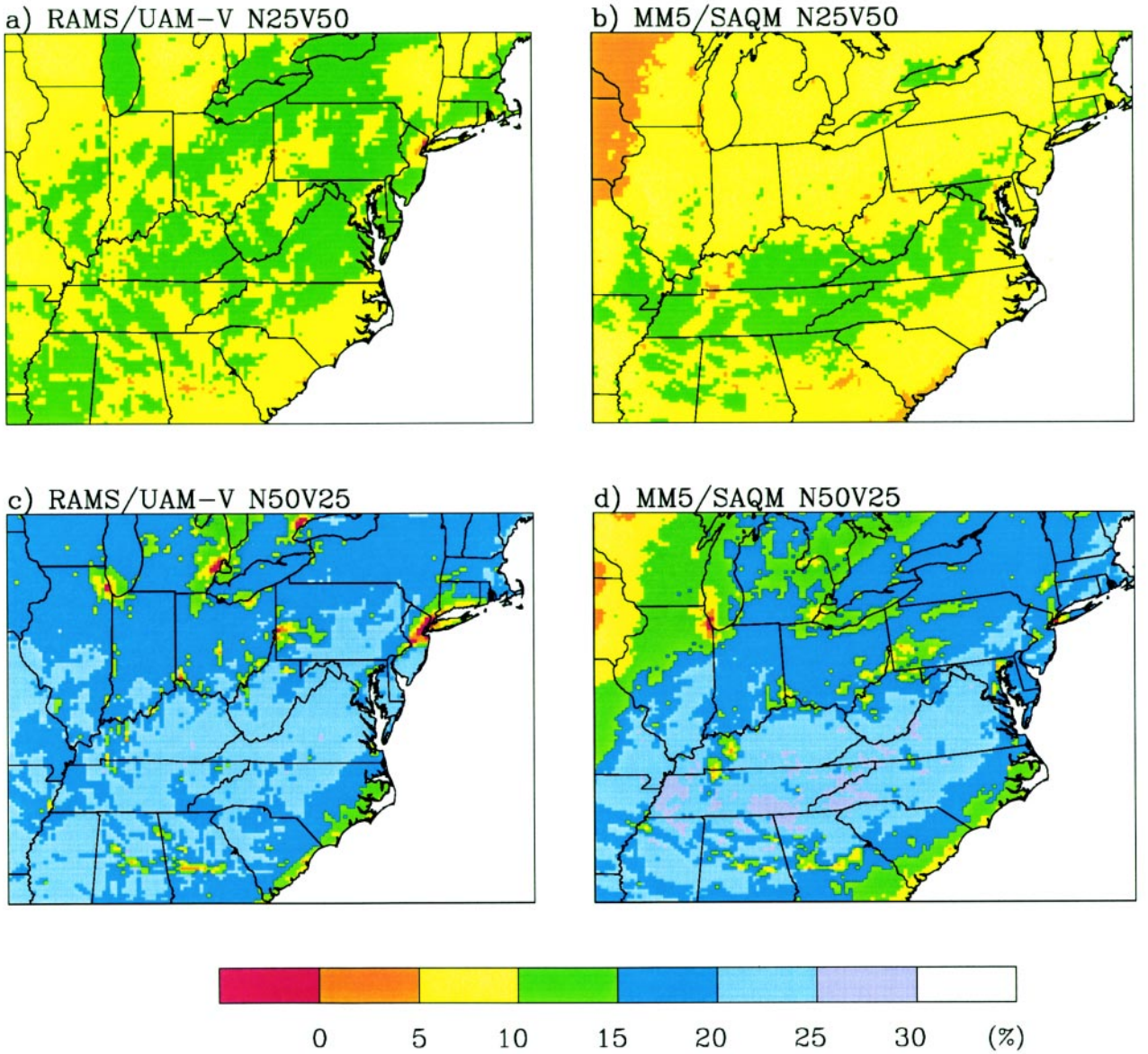

FIG. 8. Average index of improvement (%) in hourly averaged maximum ozone concentrations over the analysis grid for the eight episode days. Percentages less than or equal to zero imply no improvement or worsening. [(a), (b)] Index of improvement in ozone from the base case (NOOVOO) with respect to the VOC-focused (N25V50) scenario for RAMS/UAM-V and SAQM, respectively. [(c), (d)] Index of improvement in ozone from the base case (NOOVOO) with respect to the NO_x-focused (N50V25) scenario for RAMS/UAM-V and SAQM, respectively.

urban and coastal areas, while major portions of the interior rural regions have a CV of less than 30%. However, subtle differences are apparent between the two models at individual grid cells. For example, in the case of New York City and its neighboring areas, the VOC-focused control shows variability of 70% or higher compared to 20% or less in the case of SAQM (see Figs. 9a,b). A similar feature is also evident over the Washington D.C. region and a few of the other areas, suggesting that the day-to-day variability in the predicted ozone improvement is more pronounced in the case of UAM-V than SAQM. A similar conclusion can be drawn from the spatial distributions for the NO_x-focused scenario (see Figs. 9c,d).

Although both models show similar direction in terms of change in ozone levels due to emission controls, the variability in the magnitudes of actual ozone improvements (i.e., relative changes) predicted at a grid cell are very different. Thus, there are differences in the efficacy of both VOC- and NO_x-focussed emis-

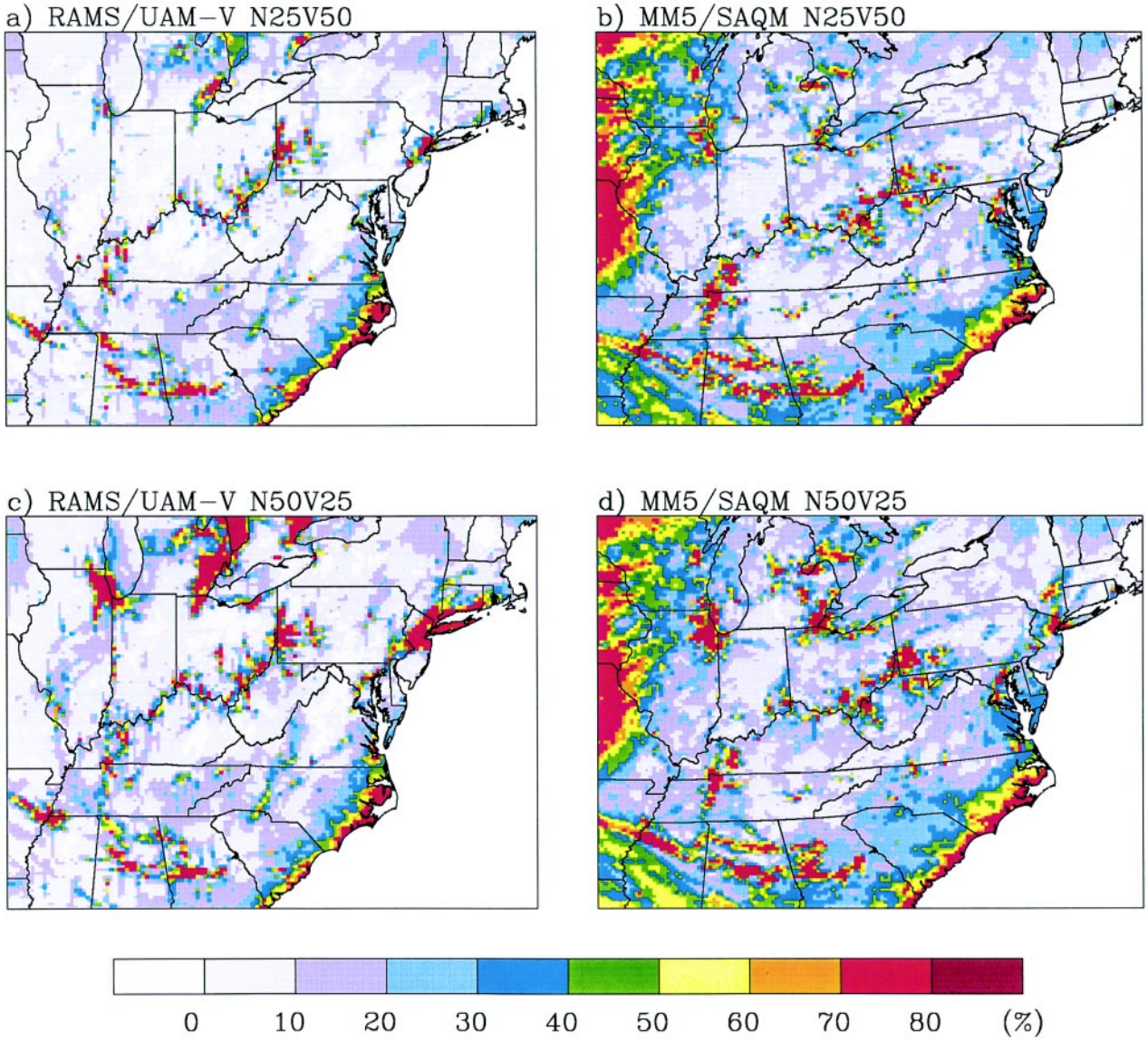

FIG. 9. Coefficient of variation (CV) (%) defined as the ratio of the standard deviation to the mean of the index of improvement over the three episodes. [(a), (b)] The CV based on the standard deviation and mean of the index of improvement in ozone from the base case (N00V00) with respect to the VOC-focused (N25V50) scenario for RAMS/UAM-V and MM5/SAQM, respectively. [(c), (d)] The CV based on the standard deviation and mean of the index of improvement in ozone from the base case (N00V00) with respect to the NO_x-focused (N50V25) scenario for RAMS/UAM-V and MM5/SAQM, respectively.

sions reductions between the two modeling systems at individual grid cells on individual days, even though the models were simulated with a common emissions database and chemical mechanism. An examination of the cumulative distribution of the index of improvement (not shown) under the NO_x-focused scenario indicates that for a 15% ozone improvement over the analysis domain, the percentage of grid cells that show improvement is about 40% for SAQM and is 60% for UAM-V. For the VOC-focused scenario, for a 10% index of improvement, the percentage of grid cells showing improvement is about 10% in the case of SAQM, whereas it is about 35% in the case of UAM-V. Also, both models are found to respond differently when consideration is given to the magnitude of cells not improving: less than 5% of the grid cells in the case of UAM-V versus about 10% for SAQM. However, if the index of improvement is considered at the locations where the 489 monitors are, then the differences between the cumulative distributions to the

two modeling systems are found to be principally limited to those locations that do not show improvement under the NO_x-focused scenario, which compose less than 1% of the monitors.

The above results suggest that even if the two modeling systems were to "pass" the operational model performance criteria, there could be differences in the magnitude of improvement in ozone at some grid cells. However, these differences are found to be reduced when consideration is given to the level of improvement in ozone at the monitoring locations only. These differences between the two models can be attributed to the formulation and application of the photochemical modeling systems since the emissions data and the chemical mechanism are kept the same. These results are similar to those reported by Biswas and Rao (2001) and Biswas et al. (2000), who reported the results of a single Eulerian photochemical model driven with two meteorological drivers.

5. Summary

In this paper, we examined the performance of two ozone modeling systems, RAMS/UAM-V and MM5/SAQM, in predicting the observed ozone air quality for three elevated ozone events of 1995. The meteorological features associated with these three high-ozone episodes in the eastern United States include the presence of a slow-moving high pressure system, westerly and southwesterly low-level jets, stable boundary layers, and the Appalachian lee-side trough. The response of the modeling systems to hypothetical emission reductions is assessed through VOC- versus NO_x-focused controls.

The results of ozone predictions for the three episodes reveals that the two modeling systems exhibit differences in their temporal and spatial ozone patterns for individual episode days at individual grid cells even though they utilized the same emissions database. However, the modeling systems were found to yield a similar level of operational performance when model outputs are averaged over all episode days. Even though both modeling systems were responding directionally similarly, they predicted different responses to emission reductions in terms of the magnitude of ozone improvement at individual grid cells on individual days. Since both modeling systems used the same emissions inventory and chemical mechanism, the differences between the models' response to emission reductions are attributable to the differences in the formulation of the Eulerian photochemical models and meteorological fields. However, these differences between the two models can be reduced when all episode days are averaged. Thus, our results lend further support to the recent EPA guidance (1999) regarding the use of daily maximum ozone concentrations averaged over all episode days simulated for regulatory purposes.

Acknowledgments. This research is supported in part by the U.S. Environmental Protection Agency under STAR Grant R825260-01-0, EPRI under Contract WO3189-12, New York State Energy Research and Development Authority under Contracts 4914 and 6085, and by the New York State Department of Environmental Conservation. Thanks are extended to Nianjun Zhou, Shiang-Yuh Wu, and Eric Zalewsky for their work in the initial stages of this study. We also would like to express our thanks to Dr. Steve Hanna for his constructive comments on the paper. The views and policies expressed in this paper do not necessarily reflect those of the sponsors or of the New York State Department of Environmental Conservation.

References

Berman, S., J. Y. Ku, J. Zhang, and S. T. Rao, 1999: Spatial and temporal variation of the mixing depth over the northeastern United States during summer of 1995. *J. Appl. Meteor.,* **38,** 1661–1673.

Biswas, J., and S. T. Rao, 2001: Uncertainties in episodic ozone modeling stemming from uncertainties in the meteorological fields. *J. Appl. Meteor.,* **40,** 117–136.

——, ——, N. Seaman, and K. Zhang, 2000: Sensitivity of the regional ozone modeling results to different physical processes within a meteorological model. *Proc. 11th Joint Conf. on the Applications of Air Pollution Meteorology,* Long Beach, CA, Amer. Meteor. Soc. and the Air and Waste Management Association, 121–126.

Blackadar, A. K., 1979: High resolution models of the planetary boundary layer. *Advances in Environmental Science and Engineering,* J. R. Pfafflin and E. N. Ziegler, Eds., Gordon and Breach Science Publications, 50–85.

Brankov, E., S. T. Rao, and P. S. Porter, 1998: A trajectory-clustering-correlation methodology for examining the long-range transport of air pollutants. *Atmos. Environ.,* **32,** 1525–1534.

Carter, W. P. L., 1996: Condensed atmospheric photoxidation mechanism for isoprene. *Atmos. Environ.,* **30,** 4275–4290.

Chameides, W. L., R. D. Saylor, and E. B. Cowling, 1997: Ozone pollution in the rural U.S. and the new NAAQS. *Science,* **276,** 916.

Chang, J. S., S. Jin, Y. Li, M. Beauharnois, C.-H. Lu, H.-C. Huang, S. Tanrikulu, and J. DaMassa, 1997: The SARMAP Air Quality Model. Final Rep. California Air Resources Board, California Environmental Protection Agency, Sacramento, CA, 109 pp.

Clarke, J. F., and J. K. S. Ching, 1983: Aircraft observations of regional transport of ozone in the northeastern United States. *Atmos. Environ.,* **17,** 1703–1712.

Deuel, H. P., G. Z. Whitten, and J. L. Haney, 1996: Memorandum: Implementation of an updated isoprene chemistry mechanism in photochemical models using the CB-IV chemical mechanism, ICF Kaiser Consulting Group, San Rafael, CA, 3 pp.

Dickinson, R. E., A. Henderson-Sellers, P. J. Kennedy, and M. F. Wilson, 1986: Biosphere–Atmosphere Transfer Scheme (BATS) for the NCAR Community Climate Model, NCAR Tech. Note TN-275+STR, 69 pp.

EPA, 1991: Guideline for regulatory applications of the Urban Airshed Model. U.S. Environmental Protection Agency Report EPA-450/4-91-013, EPA, Office of Air Quality Planning and Standards, Research Triangle Park, NC, 89 pp.

——, 1997: National Ambient Air Quality Standards for Ozone: Proposed decision. *Fed. Regist.,* **61,** 65 717–65 750.

——, 1999: Draft guidance on the use of models and other analyses in attainment demonstration for the 8-hour ozone NAAQS. U.S. Environmental Protection Agency Rep. EPA-454/R/99-004, 157 pp.

Geron, C. D., A. B. Guenther, and T. E. Pierce, 1994: An improved model for estimating emissions of volatile organic compounds from forests in the eastern United States. *J. Geophys. Res.,* **99,** 12 773–12 791.

Gery, M., G. Z. Whitten, J. P. Killus, and M. C. Dodge, 1989: A photochemical kinematics mechanism for urban and regional scale computer modeling. *J. Geophys. Res.,* **94,** 12 925–12 956.

Grell, G. A., J. Dudhia, and D. R. Stauffer, 1994: A description of the fifth-generation Penn State/NCAR Mesoscale Model MM5. NCAR Tech. Rep., NCAR/TN-398+STR, 122 pp.

Guenther, A., P. Zimmerman, P. Harley, R. Monson, and R. Fall, 1993; Isoprene and monoterpene emission rate variability: Model evaluations and sensitivity analyses. *J. Geophys. Res.,* **98,** 12 609–12 617.

Hanna, S. R., G. E. Moore, and M. E. Fernau, 1996: Evaluation of photochemical grid models (UAM-IV, UAM-V, and the ROM/UAM-IV Couple) using data from the Lake Michigan Ozone Study (LMOS). *Atmos. Environ.,* **30,** 3265–3279.

Hogrefe, C., S. T. Rao, P. Kasibhatla, G. Kallos, C. J. Tremback, W. Hao, D. Olerud, A. Xiu, J. McHenry, and K. Alapaty, 2001a: Evaluating the performance of regional-scale photochemical modeling systems: Part I-Meteorological predictions. *Atmos. Environ.,* in press.

Hogrefe, C., S. T. Rao, P. Kasibhatla, W. Hao, G. Sistla, R. Mathur, and J. McHenry, 2001b: Evaluating the performance of regional-scale photochemical modeling systems: Part II-Ozone predictions. *Atmos. Environ.,* in press.

Kallos, G., and K. Lagouvardos, 1997: Atmospheric modeling simulations over the eastern United States with the RAMS3b model for the summer of 1995. Final Rep. to Electric Power Research Institute, Palo Alto, CA, 69 pp.

Louis, J. F., 1979: A parametric model of vertical eddy fluxes in the atmosphere. *Bound.-Layer Meteor.,* **17,** 187–202.

Lurmann, F., and N. Kumar, 1997: Evaluation of the UAM-V model performance in OTAG simulations: Summary of performance against surface observations. Rep. prepared by Sonoma Technology, Inc., for the U.S. Environmental Protection Agency/OAQPS, Research Triangle Park, NC, 116 pp.

Lyons, W. A., and H. S. Cole, 1976: Photochemical oxidant transport: Mesoscale lake-breeze and synoptic scale aspects. *J. Appl. Meteor.,* **15,** 733–743.

McNally, D. E., T. W. Tesche, C. F. Loomis, and J. G. Wilkinson, 1998: Nested regional photochemical modeling in support of the Pittsburgh–Beaver Valley ozone SIP. Preprints, *10th Joint Conf. on the Applications of Air Pollution Meteorology,* Phoenix, AZ, Amer. Meteor. Soc. and the Air and Waste Management Association, 490–494.

Michelson, S. A., and N. L. Seaman, 2000: Assimilation of NEXRAD-VAD winds in summertime meteorological simulations over the northeastern United States. *J. Appl. Meteor.,* **39,** 384–398.

Morris, R. E., M. A. Yocke, T. C. Myers, and V. Mirabella, 1992: Overview of the variable-grid Urban Airshed Model (UAM-V). *Proc. 85th Annual Meeting,* Kansas City, MO, Air and Waste Management Association, 13 pp.

——, M. A. Yocke, and T. C. Myers, 1993: Application of the nested-grid Urban Airshed Model to the Lake Michigan region. *Tropospheric Ozone: Nonattainment and Design Value Issues,* J. J. Vostal, Ed., A&WMA, 514–528.

OTAG, 1997: OTAG Technical Supporting Document. [Available online at http://www.epa.gov/ttn/rto/otag/finalrpt/].

Pagnotti, V., 1987: A mesoscale meteorological feature associated with high ozone concentrations in the northeastern United States. *J. Air Pollut. Control Assoc.,* **37,** 720–722.

Pielke, R., and M. Uliasz, 1998: Use of meteorological models as input to regional mesoscale air quality models—Limitations and strengths. *Atmos. Environ.,* **32,** 1455–1466.

Rao, S. T., I. G. Zurbenko, R. Neagu, P. S. Porter, R. F. Henry, and J. Y. Ku, 1997: Space and time scales in ambient ozone data. *Bull. Amer. Meteor. Soc.,* **78,** 2153–2166.

——, J. Y. Ku, S. Berman, K. Zhang, and H. Mao, 2001: Summertime characteristics of the boundary-layer and relationships to ozone levels over the eastern United States. *Pure Appl. Geophys.,* in press.

Russell, A., and R. Dennis, 2000: NARSTO critical review of photochemical model and modeling. *Atmos. Environ.,* **34,** 2238–2324.

Ryan, W. F., B. G. Doddridge, R. R. Dickerson, R. M. Morales, and K. A. Hallock, 1998: Pollutant transport during a regional O_3 episode in the mid-Atlantic states. *J. Air Waste Manage. Assoc.,* **48,** 786–797.

SAI, 1995: Application of UAM-V to the northeast as part of Phase I of the Modeling Ozone Cooperative (MOCA). Draft Final Rep. SYSAPP-95/049d, Systems Application International, San Rafael, CA, 289 pp.

Scheffe, R., and Morris, R. E. 1993: A review of the development and application of the urban airshed model. *Atmos. Environ.,* **27B,** 23–39.

Sistla, G., N. Zhou, W. Hao, J.-Y. Ku, S. T. Rao, R. Bornstein, F. Freedman, and P. Thunis, 1995: Effects of uncertainties in meteorological inputs on Urban Airshed Model predictions and ozone control strategies. *Atmos. Environ.,* **30,** 2011–2025.

STI, 1999: Analysis of data from the 1995 NARSTO-Northeast study. Volume V: Three-dimensional analysis of aircraft and upper-air meteorological data. Final Rep. STI-95426-1836-FR, Coodinating Research Council, Atlanta, GA, 125 pp.

Tesche, T. W., and D. E. McNally, 1997: Superregional ozone modeling and analysis study; Assessment of the reliability of the OTAG modeling system. Final Rep. AG-90/TS73 prepared for the Midwest Ozone Group, by Alpine Geophysics, LLC, Covington, KY, 98 pp.

——, P. Georgopolus, J. H. Seinfeld, F. Lurman, and P. M. Roth, 1990: Improvements in procedures for evaluating photochemical models. California Air Resources Board Rep. A832-103, Sacramento, CA, 173 pp.

Vukovich, F. M., 1995: Regional-scale boundary layer ozone variations in the eastern United States and the association with meteorological variations. *Atmos. Environ.,* **29,** 2250–2273.

Zhang, J., S. T. Rao, and S. M. Daggupaty, 1998: Meteorological processes and ozone exceedances in the northeastern United States during the 12–16 July 1995 episode. *J. Appl. Meteor.,* **37,** 776–789.

Zhang, K., and S. T. Rao, 1999: Meteorological modeling with MM5/FDDA for use in ozone studies. Part I: Mesoscale FDDA analyses on meteorological characteristics of high ozone episodes in 1995. Tech. Rep., 42 pp. [Available from New York State Department of Environmental Conservation, Albany, NY.]